Calibrations of Trumpler 20 Red Clump Stars using the Gaia G-bands

By Tiffany Zhang

Author Bio

Tiffany Zhang is a student at Great Neck South High School and has been part of her school's research program since freshman year. She is interested in astrophysics, computer science, and math. She is the co- founder, website manager, and instructor at AlphaMath, a nonprofit organization that hosts free online sessions to make learning math more accessible and fun during the pandemic. She actively participates in her school's women in STEM club SHE by hosting events and organizing fundraisers. She interned in the ReWild Long Island Summer Program to promote biodiversity, climate change resilience, and food security by reintroducing native plants to attract a variety of animals, following organic and regenerative practices of recycling and composting, and donating grown fruits and vegetables to the hungry. She qualified for AIME, represented her school in various math competitions, and participated in physics and programming competitions. The author would like to thank Dr. Shyamal Mitra, Arnav Sharma, Nicole Spinelli, and Eleanor Liu for their feedback and constant support.

Abstract

Calculating distances to astronomical objects are crucial for measuring absolute magnitude, analyzing evolution, and deriving the Hubble's constant. Different distance methods, such as main-sequence fitting and period-luminosity relations of variable stars, form the distance ladder, in which methods for shorter distances calibrate methods for larger distances. Red clump (RC) stars are not a firmly established distance indicator as the strength of their metallicity-luminosity relation varies between studies. This study investigates broader passbands for more general trends in the relation by using the G-, GBP-, and GRP-bands. Because of its substantial RC, Trumpler 20 was analyzed, and its data was collected from Gaia DR3 and Gaia-ESO DR5. The metallicity-luminosity relations demonstrated weak correlations with the highest R2 of 0.016 ($p>0.05$). However, when calculating the distance to ϵ Tauri, an RC star in the closest star cluster Hyades, the G-band metallicity-luminosity relation yielded the lowest relative error of 2.8%. This study introduces the use of Gaia photometric bands in the RC metallicity-luminosity relations to analyze different correlations for broader passbands. Future studies should further investigate broad passbands to determine if they produce significant results and narrower passbands of photometric bands that weakly correlate with metallicity.

Keywords: distance indicator, red clump, metallicity-luminosity calibration, Trumpler 20, Hyades, G-band, GBP-band, GRP-band, Gaia G-bands, distance ladder, Gaia, Gaia-ESO

Introduction

In an expanding universe, distances are crucial for calculating absolute magnitude, analyzing the evolution of astronomical objects, and deriving the Hubble constant for cosmology, strongly necessitating an improved accuracy of distance methods. Distance indicators rely on the intrinsic properties of astronomical objects and luminosity. However, each indicator can be applied in a limited range. This is because objects might not be present within certain distance ranges or become too faint outside certain distance ranges. Hence, farther distance methods rely on closer distance methods for calibration in the distance ladder. As our understanding of cosmology and evolution progresses, more accurate distance measurements can clarify and confirm the findings.

Red clump (RC) stars could be a useful distance indicator to confirm the distance calculations of other distance indicators. They are core He-burning stars with masses below the He-flash limit MHeF, or the maximum mass of a star that can have a degenerate yet He-burning core to undergo the He-flash (Girardi, 2016). Degenerate cores have similar masses, limiting the irregularity in RC luminosity and effective temperature. As a result, the RC makes up 1/3 of all red giants, creating a prominent clump in the HR Diagram (HRD) shown in Fig. 1—hence its name (Girardi, 2016). Additionally, RC stars' low mass and high metallicity create their characteristic large red convective envelope for fusion. Due to their distinguishability and high luminosity, RC stars are a promising distance indicator.

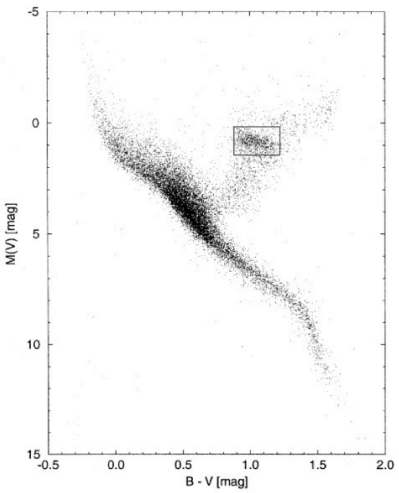

Figure 1: HR Diagram in the B and V bands using Hipparcos data. The grey box marks the red clump in the HRD. This figure is from figure 3 of Lindegren (1997) and edited by the author.

Theoretically, since the RC's luminosity increases as it transitions from mainly H-burning to He-burning over time, the RC should exhibit a metallicity-luminosity relation, which is absolute luminosity represented as a linear function of metallicity, or the concentration of all elements heavier than He relative to the Sun (Girardi, 2016). The distance can be derived by calculating the absolute magnitude from metallicity using the relation and measuring the absolute magnitude as shown

$$m - M = -5 + 5 \log d$$

where m and M are the apparent and absolute magnitudes, respectively, and d is the distance in parsecs.

However, the RC is not a firmly established distance indicator because of systematic errors and unresolved discrepancies in relationships of specific photometric bands, or passbands, with other stellar properties. For example, analyses in the V-band (500 nm - 700 nm) and I-band (700 nm - 900 nm) found unresolvable population effects, which became accepted in the research community (Pietrzyński et al., 2010; Girardi, 2016). Consequently, studies analyzed the K-band (2000 nm - 2300 nm) because of its negligible extinction, which is the dimming of observed light by dust. This was first proposed by Alves (2000) who found a weak correlation between the K-band absolute magnitude and metallicity. Grocholski & Sarajedini (2002) and Van Helshoecht & Groenewegen (2005) found comparable results and a lack of correlation of the K-band absolute magnitude with age. However, models predicted the dependence of K-band magnitudes on age and metallicity (Salaris & Girardi, 2002). These smaller trends in specific passbands may contribute to a larger and stronger trend in a broad passband to yield more accurate distance measurements.

Gaia DR3 collected the most spectrophotometric data to date with a total of 1.8 billion sources, over 1.5 billion sources of broadband photometry, and 470 million sources of their

extinctions (Vallenari et al., 2022). Gaia uses the G-band (350 nm - 1050 nm), GBP-band (330 nm - 680 nm), and GRP-band (640 nm - 1050 nm) as shown in Fig. 2, and the latter two have not yet been used for RC calibrations, despite the large influx of data in parallax and photometry.

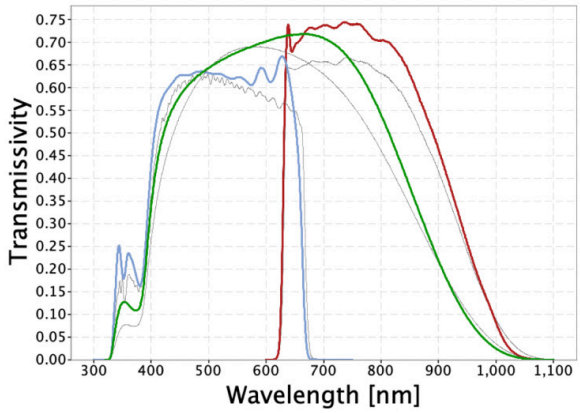

Figure 2: Gaia EDR3 photometric bands G, GBP, and GRP. The green, blue, and red lines represent the G, GBP, and GRP passbands from Gaia EDR3, respectively, and the grey lines represent the passbands before launch. This figure is from figure 24 of Riello et al. (2021).

Few studies investigated the RC in the context of the G-band. Hawkins et al. (2017) and Ruiz-Dern et al. (2017) found disagreeing results for the RC mean G-band magnitude: MG = 0.44 ± 0.01 mag and MG = 0.495 ± 0.009 mag, respectively. Moreover, Ruiz-Dern et al. (2017) analyzed different relations of the Gaia G-band absolute magnitude with metallicity, color G-KS, and effective temperature. However, the studies did not analyze a relation only between Gaia G-band absolute magnitude and metallicity.

Gaia-ESO (GES) DR5 is a large spectroscopic survey with 114,324 sources of open clusters (Gilmore, 2022). Known for its unprecedented high resolution of spectroscopic data, this survey can provide accurate metallicity measurements for the analysis of the RC (Donati et al., 2014).

Trumpler 20 (Tr 20), shown in Fig. 3, is an old open cluster located with a right ascension of 189.88° and declination of -60.63° (Donati et al., 2014; Seleznev et al., 2010). Known for its substantial RC, Tr 20 provides a good starting point for the analysis of the RC stars in the G-, GBP-, and GRP-bands with metallicity.

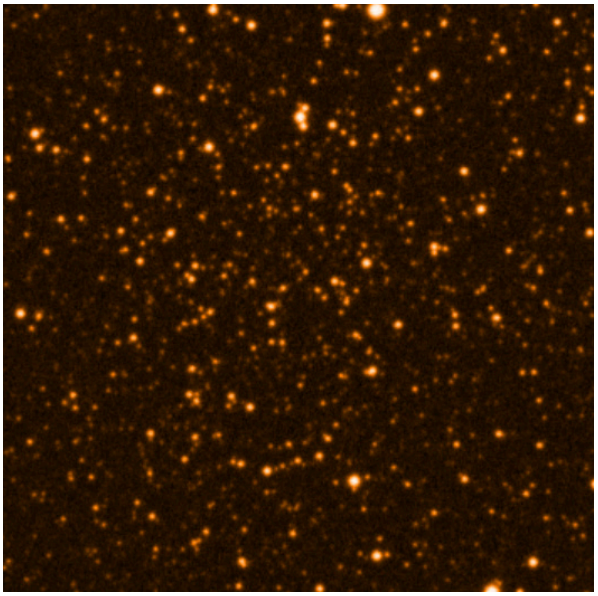

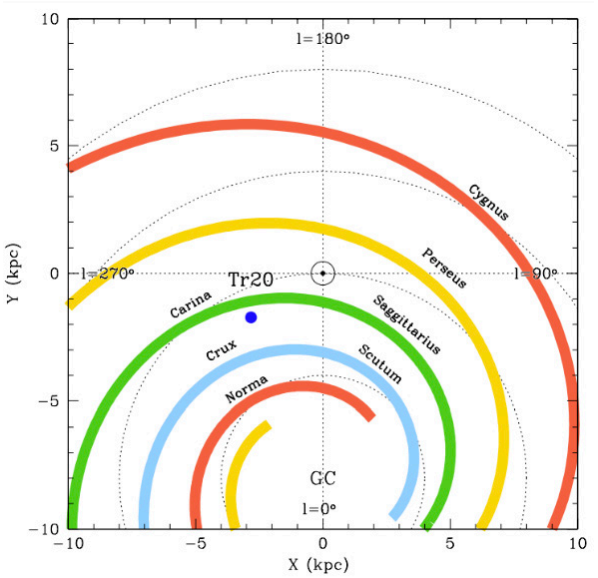

Figure 3: Trumpler 20. The figure on the left is a 10'x10' image of Trumpler 20 from the ESO Online Digitized Sky Survey, and the figure on the right is a graph of Trumpler 20's position in the Milky Way from figure 1 of Donati et al. (2014). The filled blue circle indicates the position of Tr 20 relative to the Sun and the Milky Way's spiral arms denoted by the □ symbol and colored strips, respectively.

The Hyades star cluster is the closest open star cluster. One of its RC stars is ϵ Tauri, which will be used to assess the metallicity-luminosity relation in calculating its distance (Sato et al., 2007).

The goal of this study is to analyze the metallicity-luminosity relation using a broader passband to evaluate larger trends. Section 2 details the data collection of Tr 20 and ϵ Tauri. Section 3 describes the results of the data analyses. Sections 4 and 5 contain the discussion and conclusion, respectively.

Data Collection

2.1. Trumpler 20

Data of Tr 20 was obtained from GES DR5 and Gaia DR3. The stellar parameters of right ascension, declination, and metallicity from all stars marked as members of Tr 20 were collected from GES and right ascension and declination with their respective errors, parallax, apparent magnitudes, extinctions in the G-, GBP-, and GRP-bands, and reddening E(GBP-GRP) from Gaia. Note that the reddening of light occurs due to the scattering of blue light and the passing of red light from dust. The data from Gaia was queried using the right ascension and declination range provided by Donati et al. (2014). All data with uncertainties less than -10 were considered unphysical and removed (Lindegren et al., 2018).

The data from GES and Gaia were cross-matched using right ascension and declination with their respective errors. However, data from GES did not have any measured errors, so an error of 5 arcseconds was used. Since membership was determined for stars from GES, those from Gaia were added to GES data if the rectangles formed by the errors of right ascension (ra) and declination (dec) overlapped. Objects that satisfy that condition are considered neighbors. The best neighbor is selected by the object with the smallest angular distance, calculated as

$$\cos(\theta) = \sin(\mathrm{dec}_1)\sin(\mathrm{dec}_2) + \cos(\mathrm{dec}_1)\cos(\mathrm{dec}_2)\cos(\mathrm{ra}_1 - \mathrm{ra}_2)$$

where θ represents the angular distance, ra1 and dec1 are the right ascension and declination of one object, and ra2 and dec2 are those of the other.

The data were filtered by removing data outside of ±2 standard deviations of both parallax and intrinsic color (GBP-GRP)0, which is calculated as shown

$$(G_{\mathrm{BP}} - G_{\mathrm{RP}})_0 = G_{\mathrm{BP}} - G_{\mathrm{RP}} - E(G_{\mathrm{BP}} - G_{\mathrm{RP}})$$

where GBP and GRP are the GBP- and GRP-band absolute magnitudes, respectively.
Color-magnitude diagrams (CMD) were created to isolate the RC. The absolute magnitude of each photometric band MG, MBP, and MRP was calculated using

$$m - M = -5 + 5\log\left(\frac{1}{p}\right) + A$$

where p is the parallax, A is the extinction, and m and M are the apparent and absolute magnitudes, respectively. The CMD was plotted for each photometric band, and the RC's absolute magnitude and color ranges were determined to isolate the data as shown in Fig. 4. Note that the isolated RC stars are the same amongst the different CMDs, which is expected and helps reinforce the validity of this sample. The data were filtered for outliers by removing data outside of ±2 standard deviations for both parallax and metallicity. The properties of the resulting 84 RC stars are described in Table 1.

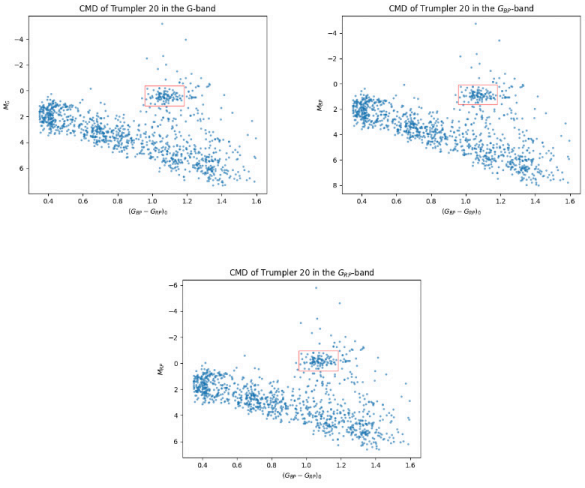

Figure 4: CMD of Trumpler 20 red clump in the G-band. The intrinsic color and absolute magnitude were calculated using Equations 1 and 2, respectively.

The RC is marked by the red rectangle and later isolated using its magnitude and color range.

Table 1. Description of Trumpler 20 Red Clump Stars' Properties. After the data of the RC was isolated and filtered (n=84), the mean, median, and standard deviations of the absolute magnitudes in the G-, GBP-, and GRP-bands, intrinsic color, and metallicity were calculated as shown in the table below. The errors for the mean represent ±1 SEM.

Trumpler 20 Red Clump Stars

	M_G	M_{BP}	M_{RP}	$(G_{BP}-G_{RP})_0$	[Fe/H]
Mean	0.46	0.91	-0.16	1.07	0.07
Median	0.50	0.93	-0.13	1.07	0.08
Standard deviation	0.28	0.28	0.28	0.04	0.11

2.2. ϵ Tauri

ϵ Tauri (HIP 20889) is one of the RC stars in the Hyades cluster (Sato et al., 2007). Its stellar parameters are listed in Table 2. The metallicity was obtained from Table 1 by Sato et al. (2007), and the rest of the properties from Gaia. The intrinsic color and magnitudes were calculated using Equations 1 and 2, respectively.

Table 2. Stellar Parameters of ϵ Tauri Hyades Red Clump Star. The metallicity was obtained from Sato et al. (2007), and the rest of the data (right ascension, declination, and parallax with its respective errors, apparent magnitudes, and extinctions in the G-, GBP-, and GRP-bands, and reddening E(GBP-GRP)) was queried from Gaia. The intrinsic color and magnitudes in each photometric band (G, GBP, and GRP) were calculated using Equations 1 and 2, respectively.

Stellar Parameters of ϵ Tauri

Parameter	Value
Parallax (mas)	22.37 ± 0.17
M_G	0.028
M_{BP}	0.65
M_{RP}	-0.59
$(G_{BP}-G_{RP})_0$	1.24
[Fe/H]	0.17 ± 0.04

Data Analysis

3.1. Regressions of Metallicity-Luminosity Relations

Using the data of the isolated RC, the absolute magnitude was plotted as a function of metallicity. Linear regressions were fitted in the three photometric bands shown in Fig. 8. All the regressions have low R2 values, suggesting a weak correlation, and were statistically similar to the null hypothesis where no correlation is present (p>0.05).

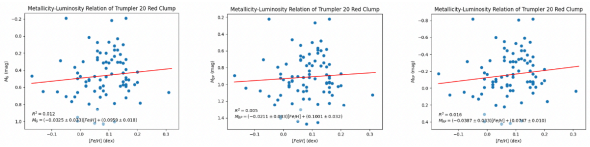

Figure 5: Linear regressions of metallicity-luminosity relation from the RC of Trumpler 20. The linear regression for the G-, GBP-, and GRP-bands are represented by the red line, and its equation and R2 are shown. Errors in the regression represent ±1 standard deviation.

To evaluate the validity of the calibration, the root mean square errors (RMS) were listed in Table 3 and calculated using

$$RMS = \sqrt{\frac{\sum_{i=1}^{N}(x_{\text{measured}} - x_{\text{estimated}})^2}{N}}$$

where N is the sample size. Of the three calibrations, the GBP-band calibration exhibits the greatest RMS of 0.858 while the GRP-band calibration exhibits the least RMS of 0.350.

Hence, in all three photometric bands, a constant RC mean magnitude can be assumed and used to estimate distance, so this was evaluated as a distance method as well. Note that these absolute magnitudes are pairwise significantly different by t-tests (p<0.05). These differences in mean magnitude between different passbands are expected and help reinforce the validity of the sample.

Table 3. Root mean square errors of metallicity-luminosity relations. The RMS of each metallicity-

luminosity relation was calculated using Equation 3.

Root Mean Square Errors			
	G-band	G_{BP}-band	G_{RP}-band
RMS	0.457	0.858	0.350

3.2. Comparing Actual Distances with Calculated Distance

To assess the consistency of the distance calculations relative to the distances measured by Gaia, the derived distances of the Tr 20 RC from each passband calibration and mean magnitude were plotted against actual distances calculated using parallax measurements from Gaia in Fig. 6 and 7, respectively. Equation 2 was used to calculate the distance for the estimated magnitude from the calibrations. The solid black line represents the identity line, and the dotted lines represent it shifted vertically by ±1 RMS of the distances, which was calculated using Equation 3.

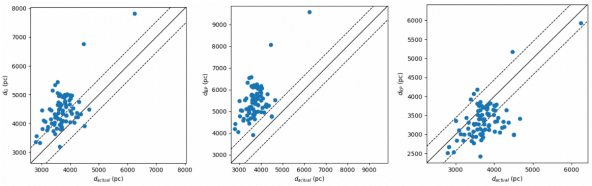

Figure 6: Actual distance vs. estimated distance plots of the metallicity-luminosity calibrations. The G-, GBP-, and GRP-band metallicity-luminosity calibrations were used to calculate the estimated distance for the left, middle, and right plots, respectively. The actual distance was calculated using parallax measurements from Gaia. The solid diagonal line represents the identity line, and the dotted lines represent ±1 RMS, which was calculated using Equation 3

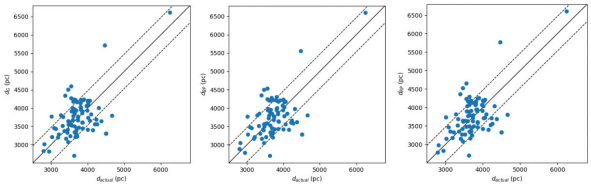

Figure 7: Actual distance vs. estimated distance plots of the mean magnitudes. The G-, GBP-, and GRP-band mean magnitudes from Table 1 were used to calculate the estimated distance for the left, middle, and right plots, respectively. The actual distance was calculated using parallax measurements from Gaia. The solid diagonal line represents the identity line, and the dotted lines represent ±1 RMS, which was calculated using Equation 3.

3.3. Distance Estimations to ϵ Tauri

To assess the accuracy of the distance methods, the absolute magnitude estimates were calculated and the obtained apparent magnitudes and extinctions from Gaia were used to derive distances using Equation 4. All the calculated distances were compiled in Table 4. The relative errors (RE) were calculated as a percent using

$$\mathrm{RE} = \frac{|d_{\mathrm{actual}} - d_{\mathrm{calculated}}|}{d_{\mathrm{actual}}}$$

where dactual and dcalculated are the actual and calculated distances, respectively. The distance calculated using the G-band calibration resulted in the smallest RE of 2.8% while using the GRP-band calibration resulted in the largest RE of 26.1% in Table 4.

Table 4. Distance estimates to ϵ Tau. Using the parallax measurement from Gaia, the true distance is 44.71 pc. Estimates of the absolute magnitude in each photometric band were derived with the regressions and metallicity and used to calculate distance using Equation 4. Since the linear regressions cannot reject the null hypotheses (p>0.05), a mean absolute magnitude was assumed and used to estimate distance as well. The relative errors (RE) of each calculated distance were derived as a percent using Equation 5.

Distances to ϵ Tau						
	G-band	RE_G	G_{BP}-band	RE_{BP}	G_{RP}-band	RE_{RP}
Mean magnitude	36.65	18.0%	39.61	11.4%	36.68	18.0%
Linear regression	43.45	2.8%	39.6	11.4%	33.02	26.1%

Discussion

The goal of this study is to analyze the metallicity-luminosity relation in the context of a broader passband, specifically the G-, GBP-, and GRP-

bands, for a larger trend.

4.1. Analysis of Calibration Data

The metallicity-luminosity relations of RC stars in the Gaia photometric bands G, GBP, and GRP demonstrated insignificant and weak correlations ($p>0.05$) as shown in Fig. 8. The GBP-band calibration exhibited the weakest correlation and largest RMS, which is inconsistent with Bilir et al. (2013) where the V-band (500 - 700 nm) magnitude, which composes half of the GBP-band wavelength range, strongly correlated with metallicity ($R = 0.971$). Tr 20's large distance possibly caused the discrepancy, increasing the possibility of obscuration by dust, and GBP-band range's short wavelengths, causing greater sensitivity to extinction and scattering. Moreover, studies found that the I-band (700 - 900 nm), which composes half of the GRP-band wavelength range, and V-band magnitudes are susceptible to unresolvable population effects (Pietrzyński et al., 2010). As a result, the G-band composing of the GBP- and GRP-bands' wavelength ranges may have caused its lack of correlation.

Because of the insignificant regression results, the mean magnitudes were evaluated as distance methods. This study found a mean RC G-band magnitude of $MG = 0.46 \pm 0.28$ mag as presented in Table 1, which is consistent with Hawkins et al. (2017) who found $MG = 0.44 \pm 0.01$ mag and with Ruiz-Dern et al. (2017) $MG = 0.495 \pm 0.009$ mag, but only because of the large error. This large spread of the G-band magnitudes is likely due to the sampling of one cluster.

4.2. Applicability of Calibration and Mean Magnitudes

To assess the reliability of distance calculations with the mean magnitudes and metallicity-luminosity calibrations, both actual distance vs. calculated distances graphs and distance estimations to ϵ Tauri were used.

The actual distance vs. calculated distance graphs for the calibrations exhibited systematic tendencies as shown in Fig. 9, especially for the GBP-band where most of the stars were skewed towards greater distances and only two of the stars fell inside ±1 RMS from the identity line. The distance estimations by the G-band calibration were also skewed to greater distances while those by the GRP-band calibration were skewed to closer distances. This was probably due to uncorrected systematic errors in extinction or reddening as the susceptibility of each wavelength varies. However, the actual distance vs. calculated distance graphs for the mean magnitudes exhibited no systematic tendencies as most of the points fall within ±1 RMS from the identity line. This may have occurred because the mean fits the systematic tendencies of the data. Hence, these distance methods must also be evaluated with other stars that are not part of the sample to assess their reliabilities.

The Hyades RC star ϵ Tauri was used to evaluate the validity of these distance methods. As presented in Table 4, the GRP-band calibration calculation exhibited the highest RE of 26.1%, while the G-band calibration calculation exhibited the lowest RE of 2.8%. The calculated distances from mean magnitudes were found to have REs smaller than 20% but are less accurate than the distance calculated with the G-band calibration. Using the mean G-band magnitudes from Hawkins et al. (2017) and Ruiz-Dern et al. (2017), the calculated distance to ϵ Tauri is 36.99 pc and 36.06 pc, which were 0.9% greater and 1.6% less than that calculated using this study's mean G-band magnitude. However, the calculated distance using the G-band calibration was relatively more accurate than using G-band mean magnitude as used by previous studies.

4.3. Limitations and Future Research

The data collected was susceptible to various systematic errors. Since Tr 20 is a rather distant open star cluster, the small parallax measurements can be easily influenced by parallax errors. Moreover, the position of Tr 20 makes it susceptible to pollution by unwanted stars in the CMD (Donati et al., 2014). Unaccounted extinction and reddening may also have contributed to systematic errors since the photometric bands used in this study are easily obscured by dust.

The analysis of larger passbands produces moderately weak results because the various smaller trends seem to strongly influence it, so an overall trend was not apparent. This result may be similar to the

weak correlation between metallicity and luminosity in specific photometric bands caused by analyzing too broad a range of wavelengths that should be broken down into smaller ranges for analysis. For instance, one past study clarified the relation of RC stars with luminosity, metallicity, and age in the K-band by separating them by age: in older RCs (>~2 Gyr), the K-band magnitude was shown to be sensitive to age but not metallicity while in younger RCs (<~2 Gyr), the K-band magnitude was shown to be sensitive to metallicity but not age (Grocholski & Sarajedini, 2001).

Future research should continue investigating novel calibrations, especially those that look at more detailed trends rather than overall trends. Other stellar parameters can be analyzed similarly to the age analysis by Grocholski & Sarajedini (2001) to uncover more detailed trends. Additionally, analyzing an entire spectrum of wavelengths to reveal trends of different smaller wavelength ranges can possibly determine the optimal wavelength range in which a metallicity-luminosity relation is strongest. However, studies should also clarify the RC luminosity relations in the G-, GBP-, and GRP-bands by collecting data from a variety of star clusters and analyzing various parameters to improve correlation and significance.

Conclusion

The goal of this study was to analyze the metallicity-luminosity relation in larger passbands to analyze overall trends in luminosity. The relations in the G-, GBP-, and GRP-bands exhibited weak correlation and statistical equivalence with the null hypotheses ($p>0.05$). Moreover, systematic tendencies in distance calculations were observed in each band, particularly the GBP-band. This suggests that smaller photometric trends strongly influenced larger photometric trends, so future research should investigate smaller and more detailed trends, especially for photometric bands that demonstrate a weak correlation. However, the distance calculated from the metallicity-luminosity relation in the G-band to ϵ Tauri had a low RE, better than using the mean magnitude G-band magnitude as implemented by previous studies, so other relations in the G-band should be explored. These results set a new path in the calibration of the RC's luminosity relations to derive more accurate distance measurements for calibration in the distance ladder.

References

Alves, D. R. (2000). K-band calibration of the red clump luminosity. The Astrophysical Journal, 539(2), 732.

Bilir, S., Ak, T., Ak, S., Yontan, T., & Bostancı, Z. F. (2013). A new absolute magnitude calibration for red clump stars. New Astronomy, 23, 88-97.

Cannon, R. D. (1970). Red giants in old open clusters. Monthly Notices of the Royal Astronomical Society, 150(1), 111-135.

Donati, P., Gaudin, T. C., Bragaglia, A., Friel, E., Magrini, L. A. U. R. A., Smiljanic, R., ... & Maiorca, E. (2014). The Gaia-ESO Survey: Reevaluation of the parameters of the open cluster Trumpler 20 using photometry and spectroscopy. Astronomy & Astrophysics, 561, A94.

Gilmore, G. (2022). ESO public survey programme Gaia-ESO spectroscopic survey, Data Release DR5. ESO. https://www.eso.org/rm/api/v1/public/releaseDescriptions/191.

Girardi, L. (2016). Red clump stars. Annual Review of Astronomy and Astrophysics, 54(1), 95-133.

Grocholski, A. J., & Sarajedini, A. (2002). WIYN open cluster study. X. The K-band magnitude of the red clump as a distance indicator. The Astronomical Journal, 123(3), 1603.

Hawkins, K., Leistedt, B., Bovy, J., & Hogg, D. W. (2017). Red clump stars and Gaia: calibration of the standard candle using a hierarchical probabilistic model. Monthly Notices of the Royal Astronomical Society, 471(1), 722-729.

Lindegren, L., Hernández, J., Bombrun, A., Klioner, S., Bastian, U., Ramos-Lerate, M., ... & Vecchiato, A. (2018). Gaia data release 2-the astrometric solution. Astronomy & Astrophysics, 616, A2.

Lindegren, L., Kovalevsky, J., Hoeg, E., Bastian, U., Bernacca, P. L., Crézé, M., ... & Petersen, C. S. (1997). The Hipparcos catalogue. Astronomy and

Astrophysics, 323(1), 49-52.

Paczyński, B., & Stanek, K. Z. (1998). Galactocentric distance with the OGLE and Hipparcos red clump stars. The Astrophysical Journal, 494(2), L219.

Pietrzyński, G., Górski, M., Gieren, W., Laney, D., Udalski, A., & Ciechanowska, A. (2010). The Araucaria project. Population effects on the V-and I-band magnitudes of red clump stars. The Astronomical Journal, 140(4), 1038.

Riello, M., De Angeli, F., Evans, D. W., Montegriffo, P., Carrasco, J. M., Busso, G., ... & Yoldas, A. (2021). Gaia Early Data Release 3-Photometric content and validation. Astronomy & Astrophysics, 649, A3.

Ruiz-Dern, L., Babusiaux, C., Arenou, F., Turon, C., & Lallement, R. (2018). Empirical photometric calibration of the Gaia red clump: Colours, effective temperature, and absolute magnitude. Astronomy & Astrophysics, 609, A116.

Salaris, M., & Girardi, L. (2002). Population effects on the red giant clump absolute magnitude: the K band. Monthly Notices of the Royal Astronomical Society, 337(1), 332-340.

Sato, B. E., Izumiura, H., Toyota, E., Kambe, E., Takeda, Y., Masuda, S., ... & Ida, S. (2007). A planetary companion to the Hyades giant ϵ Tauri. The Astrophysical Journal, 661(1), 527.

Seleznev, A. F., Carraro, G., Costa, E., & Loktin, A. V. (2010). Homogeneous photometry and star counts in the field of 9 Galactic star clusters. New Astronomy, 15(1), 61-75.

Vallenari, A., Brown, A. G. A., Prusti, T., de Bruijne, J. H. J., Arenou, F., Babusiaux, C., ... & Bianchi, L. (2022). Gaia Data Release 3: Summary of the content and survey properties. arXiv preprint arXiv:2208.00211.

Van Helshoecht, V., & Groenewegen, M. A. T. (2007). K-band magnitude of the red clump as a distance indicator. Astronomy & Astrophysics, 463(2), 559-565.